Inorganic Chemistry

Article

pubs.acs.org/IC

Experimental and Computational Study on the Structure and Properties of Herz Cations and Radicals: 1,2,3-Benzodithiazolium, 1,2,3-Benzodithiazolyl, and Their Se Congeners

Alexander Yu. Makarov,*[,†] Frank Blockhuys,*[,‡] Irina Yu. Bagryanskaya,[†] Yuri V. Gatilov,[†] Makhmut M. Shakirov,[†] and Andrey V. Zibarev*[,†,§]

[†]Institute of Organic Chemistry, Siberian Branch of the Russian Academy of Sciences, 630090 Novosibirsk, Russia

[‡]Department of Chemistry, University of Antwerp, Universiteitsplein 1, B-2610 Antwerp, Belgium

[§]Department of Physics, National Research University—Novosibirsk State University, 630090 Novosibirsk, Russia

Supporting Information

ABSTRACT: Salts of 1,2,3-benzodithiazolium (**1**), 2,1,3-benzothiaselenazolium (**3**), and 1,2,3-benzodiselenazolium (**4**) (Herz cations), namely, [**1**][BF_4], [**1**][$SbCl_6$], [**3**][BF_4], [**3**][$GaCl_4$], [**3**][$SbCl_6$], and [**4**][$GaCl_4$], were prepared from the corresponding chlorides and $NaBF_4$, $GaCl_3$, or $SbCl_5$. It was found that [**1**][$SbCl_6$] and [**3**][$SbCl_6$] spontaneously transform in MeCN solution to [**1**]$_3$[$SbCl_6$]$_2$[Cl] and [**3**]$_3$[$SbCl_6$]$_2$[Cl], respectively. [**1**][BF_4], [**1**]$_3$[$SbCl_6$]$_2$[Cl], [**3**][BF_4], [**3**]$_3$[$SbCl_6$]$_2$[Cl], and [**4**][$GaCl_4$] were structurally characterized by X-ray diffraction (XRD). In solution, these $[BF_4]^-$ and $[GaCl_4]^-$ salts as well as [**1**][$GaCl_4$], [**2**][$GaCl_4$], [**3**][$GaCl_4$], [**3**][Cl], and [**4**][Cl] were characterized by multinuclear nuclear magnetic resonance (NMR). The corresponding Herz radicals **1**$^\bullet$**−4**$^\bullet$ were obtained in toluene and DCM solutions by the reduction of the appropriate salts with Ph_3Sb and characterized by EPR. Cations **1**−**4** and radicals **1**$^\bullet$**−4**$^\bullet$ were investigated computationally at the density functional theory (DFT) and second-order Møller−Plesset (MP2) levels of theory. The B1B95/cc-pVTZ method was found to satisfactorily reproduce the experimental geometries of **1**−**4**; an increase in the basis set size to cc-pVQZ results in only minor changes. For both **1**−**4** and **1**$^\bullet$**−4**$^\bullet$, the Hirshfeld charges and bond orders, as well as the Hirshfeld spin densities for the radicals, were calculated using the B1B95/cc-pVQZ method. It was found for both the cations and the radicals that replacing S atoms with Se atoms leads to considerable changes in the atomic charges, bond lengths, and bond orders only at the involved and the neighboring sites. According to the calculations, 60% of the positive charge in the cations and 80% of the spin density in the radicals is localized on the heterocycles, with the spin density distributions being very similar for all radicals **1**$^\bullet$**−4**$^\bullet$. For the cations **1**−**4**, the NICS values (B3LYP/cc-pVTZ for B1B95/cc-pVTZ geometries) lie in the narrow range from −5.5 ppm to −6.6 ppm for the carbocycles, and from −14.4 ppm to −15.5 ppm for heterocycles, clearly indicating the aromaticity of the cations. Calculations on radical dimers [**1**$^\bullet$]$_2$−[**4**$^\bullet$]$_2$ revealed, with only one exception, positive dimerization energies, i.e., the dimers are inherently unstable in the gas phase.

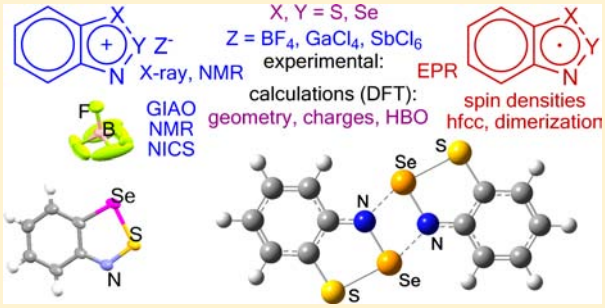

1. INTRODUCTION

1,2,3-Benzodithiazolium chlorides (or Herz salts) are an important class of reagents in many fields of pure and applied chemistry, whereas 1,2,3-benzodithiazolyls (or Herz radicals) are key intermediates for several important reactions. Normally, Herz salts are the synthetic precursors of Herz radicals, which are obtained from the salts by chemical or electrochemical reduction of the cations.[1−3] Significantly, 1,2,3-dithiazolyl and their isomeric 1,3,2-dithiazolyl derivatives, together with many other sulfur−nitrogen π-heterocyclic radicals such as 1,3,2,4- and 1,2,3,5-dithiadiazolyls, are of interest to contemporary material science as promising building blocks in the design and synthesis of molecular magnets and/or conductors. Replacement of S by Se strengthens the intermolecular interactions in the crystalline state and, consequently, increases the electrical conductivity and the magnetic exchange interactions. For instance, many selenium-containing pyridobis[1,2,3]dichalcogenazolyls are conductors and low-temperature bulk ferromagnets and canted antiferromagnets.[4−7]

In contrast to the extensively studied tricyclic 1,2,3-dichalcogenazolyls and the related cations (in which the chalcogens are S and Se),[5] the structural and electronic properties of the archetypal 1,2,3-benzodichalcogenazolyls **1**$^\bullet$**−4**$^\bullet$ and 1,2,3-benzodichalcogenazoliums **1**−**4** (Chart 1) have received relatively limited attention. For example, only cations **1** and **2** (as well as their 2-Te congener) were structurally characterized by X-ray diffraction (XRD) in the form of $[GaCl_4]^-$ salts.[1a] The geometries of cations **1** and **2** and radicals **1**$^\bullet$ and **2**$^\bullet$, as well as the capability of the former two to dimerize and the spin density distribution and isotropic hfc constants of the latter two,

Received: October 10, 2012
Published: March 19, 2013

   dx.doi.org/10.1021/ic302203t | *Inorg. Chem.* 2013, 52, 3699−3710

Chart 1

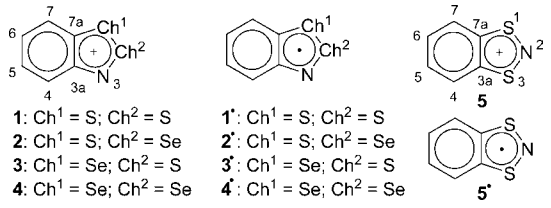

were computationally studied using density functional theory (DFT) methods.[1a] For radicals **1**•, **3**•, and **4**• hyperfine coupling and *g*-tensors were determined using pulse EPR and ENDOR spectroscopy.[3c]

For the further exploitation of Herz-type radicals in the design and synthesis of functional materials, computer-aided modeling of new species with desired properties is reasonable at the first stage. In this context, first of all, a level of computational theory providing reliable results should be established. It is necessary to emphasize that a satisfactory structural description of chalcogen−nitrogen heterocycles remains a serious challenge to computational chemistry.[9]

The present paper deals with the preparation and XRD structural characterization of the salts of cations **1**−**4** with various anions, the chemical reduction of **1**−**4** to radicals **1**•−**4**•, as well as with a computational study on both **1**−**4** and **1**•−**4**•. The latter included calculations of the molecular structures and bond orders, as well as the charge and spin density distributions. For the calculations of the bond orders, the Hirshfeld partitioning of the electron density was used, because it was found to be the best for a series of chalcogen−nitrogen systems as compared with several other approaches.[10] The same technique was applied to the calculation of the charge- and spin-density distributions. Finally, the dimerization of radicals **1**•−**4**• in the gas phase was investigated computationally. When reasonable or/and possible, a comparison with cation **5** and radical **5**• (Chart 1), isomers of **1** and **1**•, respectively, is made.

2. EXPERIMENTAL AND COMPUTATIONAL DETAILS

General Procedures. ^{1}H, ^{13}C, ^{14}N, ^{15}N, and ^{77}Se NMR spectra were recorded at the Chemical Service Center of the Siberian Branch of the Russian Academy of Sciences, using a Bruker Model DRX-500 spectrometer at frequencies of 500.13, 125.76, 36.13, 50.68, and 95.38 MHz, respectively, and a Bruker Model AV-600 spectrometer at frequencies of 600.30, 150.95, 43.36, 60.83, and 114.49 MHz, respectively, with tetramethylsilane (TMS), ammonia (NH_3; liq.) and dimethylselenide (Me_2Se) as standards; solutions in CD_3CN were used, unless otherwise indicated.

Crystallographic Analysis. Single-crystal XRD data (Table 1) were obtained using a Bruker Model P4 diffractometer for [**1**][BF_4] and [**3**][BF_4] and a Bruker Model Kappa Apex-II diffractometer for [**1**]$_3$[$SbCl_6$]$_2$[Cl], [**3**]$_3$[$SbCl_6$]$_2$[Cl], and [**4**][$GaCl_4$], with graphite-monochromated Mo Kα (0.71073 Å) radiation. The structures were solved by direct methods using the SHELXS-97 program,[11] and

Table 1. Crystal and Structure Refinement Data for [1]$_3$[$SbCl_6$]$_2$[Cl], [3]$_3$[$SbCl_6$]$_2$[Cl], [1][BF_4], [3][BF_4], and [4][$GaCl_4$]

	[**1**]$_3$[$SbCl_6$]$_2$[Cl]	[**3**]$_3$[$SbCl_6$]$_2$[Cl]	[**1**][BF_4]	[**3**][BF_4]	[**4**][$GaCl_4$]
formula	$C_{18}H_{12}Cl_{13}N_3S_6Sb_2$	$C_{18}H_{12}Cl_{13}N_3S_3Sb_2Se_3$	$C_6H_4BF_4NS_2$	$C_6H_4BF_4NSSe$	$C_6H_4Cl_4GaNSe_2$
formula weight	1167.10	1307.77	241.05	287.94	459.54
crystal system	triclinic	triclinic	monoclinic	monoclinic	monoclinic
space group	$P\bar{1}$	$P\bar{1}$	$C2/c$	$C2/c$	$P2_1/n$
a [Å]	14.9341(11)	14.1279(13)	14.6946(11)	14.769(4)	7.4699(3)
b [Å]	15.8102(10)	15.8980(13)	5.5482(4)	5.6552(15)	10.1981(3)
c [Å]	16.0843(11)	17.0527(15)	21.652(2)	21.781(5)	17.0300(6)
α [°]	87.751(4)	88.417(4)			
β [°]	85.952(4)	86.258(5)	90.309(8)	91.68(2)	93.895(1)
γ [°]	87.492(4)	88.050(5)			
V [Å^3]	3782.1(4)	3818.5(6)	1765.2(2)	1818.4(8)	1294.33(8)
Z	4	4	8	8	4
D(calc) [g/cm^3]	2.050	2.275	1.814	2.104	2.338
absorption coefficient [mm^{-1}]	2.699	2.275	0.620	4.376	8.537
F(000)	2240	2456	960	1104	856
crystal size [mm]	0.02 × 0.13 × 0.15	0.10 × 0.10 × 0.20	0.20 × 0.40 × 0.42	0.38 × 0.80 × 0.05	0.26 × 0.20 × 0.05
temperature (K)	193	173	193	193	200
θ range for data collection [°]	1.3, 28.8	1.3, 30.6	2.8, 27.0	2.8, 27.0	2.3, 32.3
index ranges	$-20 \le h \le 20$	$-20 \le h \le 20$	$0 \le h \le 18$	$0 \le h \le 18$	$-11 \le h \le 10$
	$-18 \le k \le 21$	$-22 \le k \le 22$	$5 \le k \le 7$	$-6 \le k \le 7$	$-12 \le k \le 14$
	$-21 \le l \le 21$	$-24 \le l \le 24$	$-27 \le l \le 27$	$-27 \le l \le 27$	$-25 \le l \le 25$
No. of reflections collected	194388	53761	1981	1997	25594
No. of independent reflections	19591 (R_{int} = 0.052)	22976 (R_{int} = 0.038)	1909 (R_{int} = 0.062)	1982 (R_{int} = 0.134)	4280 (R_{int} = 0.025)
observed data [$I > 2\sigma(I)$]	13643	15694	1517	1173	3648
completeness to θ [%]	99.0	97.9	99.7	99.9	92.5
min/max transmission	0.55/0.75	0.42/0.75	0.51/0.84	0.32/0.75	0.65/0.97
absorption correction	SADABS	SADABS	empirical	empirical	SADABS
No. of data/parameters	19591/757	22976/799	1909/171	1982/140	4280/127
R_1 [$I > 2\sigma(I)$]	0.0469	0.0651	0.0531	0.0709	0.0228
wR_2 (all data)	0.1111	0.1918	0.1419	0.1914	0.0532
goodness-of-fit	1.20	1.04	1.15	1.05	1.07
largest diff peak and hole (e Å^{-3})	−1.28, 1.70	−2.36, 2.95	−0.29, 0.08	−0.64, 0.66	−0.46, 0.96

dx.doi.org/10.1021/ic302203t | Inorg. Chem. 2013, 52, 3699−3710

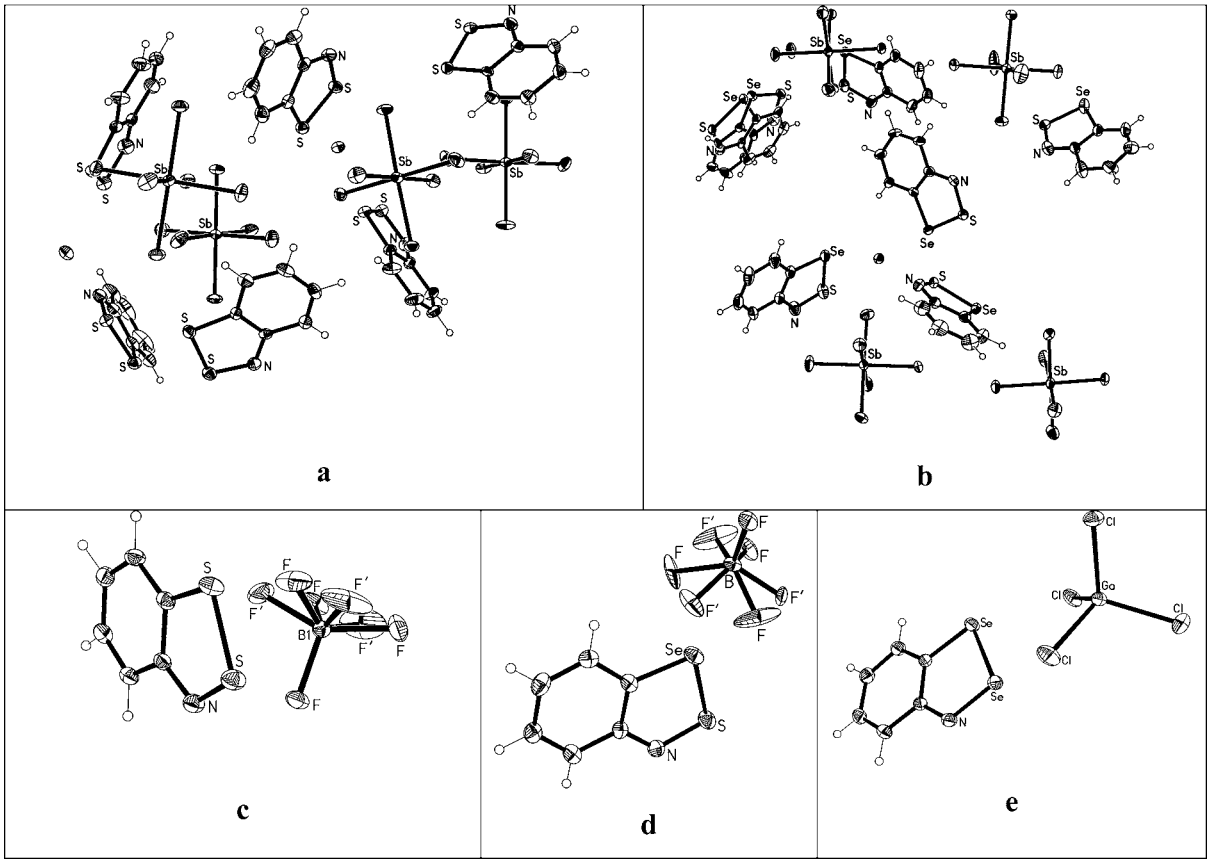

Figure 1. XRD structures of the salts (displacement ellipsoids at 30%): (a) $[\mathbf{1}]_3[SbCl_6]_2[Cl]$, (b) $[\mathbf{3}]_3[SbCl_6]_2[Cl]$, (c) $[\mathbf{1}][BF_4]$, (d) $[\mathbf{3}][BF_4]$ and (e) $[\mathbf{4}][GaCl_4]$. For selected bond lengths, see Table 3 (presented later in this paper).

refined by the least-squares method in the full-matrix anisotropic (isotropic for H atoms) approximation using the SHELXL-97 program.[11] Hydrogen atoms were located geometrically. In $[\mathbf{3}]_3[SbCl_6]_2[Cl]$, one of the six independent 2,1,3-benzothiaselenazolium cations is disordered over two positions with an occupation ratio of 0.597:0.403(5). In $[\mathbf{1}][BF_4]$ and $[\mathbf{3}][BF_4]$ three of the F atoms of the tetrafluoroborate anions are disordered over two positions with occupation ratios of 0.571:0.429(4) and 0.74:0.26(2), respectively. For $[\mathbf{3}][BF_4]$, the minor F′ atoms (Figure 1) were refined isotropically. The obtained structures were analyzed in terms of short contacts between nonbonded atoms using the PLATON[12] and MERCURY[13] programs. Atomic coordinates, thermal parameters, bond lengths, and bond angles have been deposited at the Cambridge Crystallographic Data Center as CCDC-901416 ($[\mathbf{1}]_3[SbCl_6]_2[Cl]$), CCDC-901417 ($[\mathbf{3}]_3[SbCl_6]_2[Cl]$), CCDC-901418 ($[\mathbf{1}][BF_4]$), CCDC-901419 ($[\mathbf{3}][BF_4]$), and CCDC-901420 ($[\mathbf{4}][GaCl_4]$).

EPR Measurements. EPR spectra of radicals $\mathbf{1}^{\bullet}$–$\mathbf{4}^{\bullet}$ in toluene and DCM solutions were recorded at ambient temperature using a Bruker EMX spectrometer (modulation frequency = 100 kHz, modulation amplitude = 0.01 mT). Simulations of the experimental spectra were performed using the EasySpin program.[14]

Quantum Chemical Calculations. Quantum chemical calculations were performed with the Gaussian 03 set of programs,[15] by application of standard gradient techniques at the second-order Møller–Plesset (MP2)[16] (for the geometry optimizations of the cations and radicals, and for the calculations of the hfc constants of the radicals), the DFT/B1B95[17] (for the geometry optimizations of the cations, radicals, and dimers of the radicals, for the calculations of the charge distributions and bond orders of the cations and radicals, and for the calculations of the spin-density distributions and hfc constants of the radicals), the DFT/B3LYP[18] (for the geometry optimizations of the cations and radicals, and for the calculations of the hfc constants of the radicals), the DFT/PBE[19] (for the calculation of the hfc constants of $\mathbf{1}^{\bullet}$) and the DFT/PBE0[19] (for the calculations of the hfc constants of $\mathbf{1}^{\bullet}$) levels of theory using the 6-31G(d),[20] 6-311++G(d,p),[21] cc-pVDZ,[22] cc-pVTZ,[22] and cc-pVQZ[22] basis sets; all basis sets were used as implemented in the program. Force-field calculations were used to ascertain whether the resulting C_s structures of the cations and radicals were energy minima. Dimerization energies for the radicals were calculated using the counterpoise correction implemented in Gaussian 03. Chemical shielding factors were calculated at all atomic positions and at both ring centers (nonweighted means of the heavy-atom coordinates) to obtain the NICS values, both at the B3LYP/cc-pVTZ and B3LYP/cc-pVQZ levels using the B1B95/cc-pVTZ and B1B95/cc-pVQZ geometries, respectively, using the GIAO method implemented in Gaussian 03. Chemical shifts for the C and H atoms were obtained by subtracting the chemical shielding values of these atoms from those calculated for TMS, which are 185.2231 and 31.8455 ppm, respectively, at the B3LYP/cc-pVTZ, and 183.1384 and 31.8003 ppm, respectively, at the B3LYP/cc-pVQZ level of theory. Chemical shifts for the N atoms were obtained by subtracting the chemical shielding values of these atoms from that calculated for NH_3, which is 267.5078 ppm at the B3LYP/cc-pVTZ and 263.8679 ppm at the B3LYP/cc-pVQZ level of theory. Chemical shifts for the S atoms were obtained by subtracting the chemical shielding values of these atoms from that calculated for sulfate anion (SO_4^{2-}), which is 150.8575 ppm at the B3LYP/cc-pVTZ and 174.7159 ppm at the B3LYP/cc-pVQZ level of theory. Chemical shifts for the Se atoms were obtained by subtracting the chemical shielding values of these atoms from that calculated for Me_2Se, which is 1768.1150 ppm at the B3LYP/cc-pVTZ and 1766.7785 ppm at the B3LYP/cc-pVQZ level of theory. Bond orders and charge- and spin-density distributions were calculated according to the Hirshfeld scheme.[10]

Preparations. The syntheses described below were carried out under argon and in absolute solvents. The reagents were added

dx.doi.org/10.1021/ic302203t | Inorg. Chem. 2013, 52, 3699–3710

Table 2. Analytical Data of the Salts

compound	decomposition temp [°C]	EA, found (calcd) [%] C	H	N	Cl or F	S
$[\mathbf{1}]_3[SbCl_6]_2[Cl]$	160−175	18.85 (18.52)	1.39 (1.04)	3.26 (3.60)	39.26 (39.49)	16.14 (16.48)
$[\mathbf{3}]_3[SbCl_6]_2[Cl]$	147−157	16.88 (16.53)	0.82 (0.92)	3.20 (3.21)	34.92 (35.24)	
$[\mathbf{1}][BF_4]$	135−155[a]	30.05 (29.90)	1.63 (1.67)	5.82 (5.81)	31.46 (31.53)	26.62 (26.61)
$[\mathbf{3}][BF_4]$	150−160	25.33 (25.03)	1.71 (1.40)	4.72 (4.86)	25.99 (26.39)	
$[\mathbf{3}][GaCl_4]$	150−160	17.27 (17.46)	1.01 (0.98)	3.18 (3.39)	34.70 (34.37)	
$[\mathbf{4}][GaCl_4]$	115−134	15.75 (15.68)	0.94 (0.88)	3.07 (3.05)	30.80 (30.86)	

[a]Previously reported as 165−166.5 °C.[35]

dropwise and the solvents were distilled off under reduced pressure. The physical and analytical data for the compounds synthesized are listed in Table 2.

a. [1][GaCl$_4$] and [2][GaCl$_4$]. $[\mathbf{1}][GaCl_4]$ and $[\mathbf{2}][GaCl_4]$ were prepared from $GaCl_3$ and $[\mathbf{1}][Cl]$[2,23] and $[\mathbf{2}][Cl]$, respectively, as reported previously.[1a]

b. [1][BF$_4$]. A mixture of $[\mathbf{1}][Cl]$ (949 mg, 5 mmol), $NaBF_4$ (549 mg, 5 mmol) and MeCN (5 mL) was stirred for 6 h. Then MeCN (5 mL) was added, the solution was filtered, the precipitate was washed with MeCN (25 mL) and the solvent was distilled off. The residue was dissolved in MeCN (3 mL) and Et_2O (3 mL) was added. After 9 days at 0 °C, the solution was removed with a syringe and the residue was dried in vacuo. $[\mathbf{1}][BF_4]$ was obtained in the form of elongated brown plates (613 mg, 51%) suitable for XRD.

c. [2][Cl]. Me_3SiCl (222 mg, 2.05 mmol) was added to a stirred mixture of 2-aminothiophenol (250 mg, 2.0 mmol), H_2O (18 mg, 1.0 mmol) and Et_2O (20 mL). After 40 min SeO_2 (244 mg, 2.2 mmol) and Me_3SiCl (916 mg, 8.44 mmol) were added. After an additional 24 h, the brown precipitate was filtered off, washed with Et_2O (5 × 5 mL), and dried in vacuo. $[\mathbf{2}][Cl]$ was obtained in the form of a brown powder (227 mg, 96%).

d. [3][BF$_4$]. A mixture of $[\mathbf{3}][Cl]$[24] (129 mg, 0.55 mmol), $NaBF_4$ (60 mg, 0.55 mmol), and MeCN (2 mL) was stirred for 12 h. The solution then was decanted and the precipitate was washed with MeCN (2 × 5 mL). The MeCN solutions were filtered, combined and the solvent was distilled off. The residue was recrystallized from a mixture of dichloroethane and MeCN (4:1 v/v). $[\mathbf{3}][BF_4]$ was obtained in the form of brown crystals (29 mg, 18%). Single crystals of $[\mathbf{3}][BF_4]$ suitable for XRD were grown at ambient temperature in a two-layered system (Et_2O/MeCN) under conditions of mutual diffusion of the solvents.

e. [3][GaCl$_4$]. A solution of $GaCl_3$ (96 mg, 0.54 mmol) in MeCN (1.1 mL) was added to $[\mathbf{3}][Cl]$[24] (128 mg, 0.54 mmol), and the mixture was kept at ambient temperature for 2 days. The brown solution formed was filtered and the solvent was distilled off. The crystalline residue was washed with Et_2O and recrystallized from dichloroethane. $[\mathbf{3}][GaCl_4]$ was obtained in the form of dark brown crystals (129 mg, 58%).

f. [4][GaCl$_4$]. A solution of $GaCl_3$ (178 mg, 1.0 mmol) in 2 mL of chlorobenzene was added to a stirred suspension of $[\mathbf{4}][Cl]$[24a] (287 mg, 1.0 mmol) in chlorobenzene (40 mL). After 16 h, the solution was decanted from the precipitate, 20 mL of chlorobenzene were added and the mixture was stirred for 1 h. The procedure then was repeated and the remaining solids were filtered off and washed with chlorobenzene (10 mL). All chlorobenzene solutions were combined and hexane (80 mL) was added. The precipitate formed was filtered off, washed with hexane, and dried in vacuo. $[\mathbf{4}][GaCl_4]$ was obtained in the form of a brown crystalline solid (235 mg, 51%). Single crystals of $[\mathbf{4}][GaCl_4]$ suitable for XRD were grown at ambient temperature in a two-layered system (hexane/dichloroethane), under conditions of mutual diffusion of the solvents.

g. [4][Cl] (Modified Procedure).[24a,25] (a) A solution of NaOH (3.308 g, 82.7 mmol) in H_2O (40 mL) was added to 2-nitrophenylselenocyanate[25] (1.565 g, 6.9 mmol) wetted with ethanol. Then, $Na_2S_2O_4$ (10.08 g) was added in small portions and the mixture was gently heated until a clear yellow solution formed. The mixture was cooled and acetic acid (~5 mL) was added to pH ~6. The yellow precipitate was extracted with Et_2O (4 × 10 mL), and the extract was added to a mixture of EtOH (0.5 mL), Me_3SiCl (1 mL) and Et_2O (30 mL). The yellow precipitate was filtered off, washed with Et_2O, and dried in vacuo. 2-Aminoselenophenol hydrochloride was obtained in the form of a pale yellow powder (1.179 g, 82%). (b) SeO_2 (0.637 g, 5.74 mmol) was added to a mixture of 2-aminoselenophenol hydrochloride (1.179 g, 5.65 mmol) and formic acid (15 mL) cooled in an ice bath. The brown solution formed was kept at 0 °C for 16 h; then, Et_2O (60 mL) was added and the brown precipitate was filtered off, washed with Et_2O, and dried in vacuo. $[\mathbf{4}][Cl]$ was obtained in the form of a brown powder (873 mg, 55%).

h. $[\mathbf{1}]_3[SbCl_6]_2[Cl]$ and $[\mathbf{3}]_3[SbCl_6]_2[Cl]$. $SbCl_5$ (598 mg, 0.256 mL, 2 mmol) was added to a stirred suspension of $[\mathbf{1}][Cl]$[2,23] (379.4 mg, 2 mmol) or $[\mathbf{3}][Cl]$[24] (473 mg, 2 mmol) in CH_2Cl_2 (5 mL). After 5.5 h, the precipitate was filtered off, washed with CH_2Cl_2 (2 × 2 mL), and dissolved in MeCN (2 mL). Then, Et_2O (7 mL) was layered onto the MeCN solution and the system was left at ambient temperature until the mutual diffusion of the solvents ceased. The solution was removed with a syringe and the residue was dried in vacuo. $[\mathbf{1}]_3[SbCl_6]_2[Cl]$ (202 mg, 21%) and $[\mathbf{3}]_3[SbCl_6]_2[Cl]$ (296 mg, 34%) were obtained in the form of brown-black crystals suitable for XRD.

For the electron paramagnetic resonance (EPR) measurements, radicals $\mathbf{1}^{\bullet}$−$\mathbf{4}^{\bullet}$ were prepared as follows. A solution of Ph_3Sb (2.1 mg, 7 μmol) in degassed CH_2Cl_2 (1 mL) was added to $[\mathbf{1}][Cl]$, $[\mathbf{2}][Cl]$, $[\mathbf{3}][Cl]$, or $[\mathbf{4}][Cl]$ (6 μmol). The clear solution formed was diluted with degassed CH_2Cl_2 (up to 50 mL) or evaporated using an argon stream, and degassed toluene (50 mL) was added to the residue. The solution obtained was degassed by three freeze−pump−thaw cycles and its EPR spectrum was measured.

3. RESULTS AND DISCUSSION

3.1. Herz Salts. *Preparation and XRD Characterization.* The parent salt $[\mathbf{1}][Cl]$ was prepared using methods previously described;[2,23] however, the crystals obtained were not suitable for XRD. Treatment of $[\mathbf{1}][Cl]$ with $SbCl_5$ in CH_2Cl_2, followed by crystallization of the reaction product from MeCN, gave $[\mathbf{1}]_3[SbCl_6]_2[Cl]$ (Scheme 1), whose structure was confirmed by XRD (Figure 1a). Similarly, $[\mathbf{3}]_3[SbCl_6]_2[Cl]$ was obtained from $[\mathbf{3}][Cl]$[24] (Scheme 1) and structurally characterized (Figure 1b; note that the top-left cation is disordered). For both salts, however, the experimental accuracy of the cations' geometries was rather low.

As an alternative, the anion $[BF_4]^-$ was chosen. The salts $[\mathbf{1}][BF_4]$ and $[\mathbf{3}][BF_4]$ were obtained by treatment of $[\mathbf{1}][Cl]$ or $[\mathbf{3}][Cl]$ with $NaBF_4$ in MeCN (Scheme 1), and their structures were successfully determined (Figures 1c and 1d; note that the anions are disordered). An attempt to prepare $[\mathbf{2}][BF_4]$ using this approach failed.

The final anion used was $[GaCl_4]^-$, and salts $[\mathbf{3}][GaCl_4]$ and $[\mathbf{4}][GaCl_4]$ were synthesized from $GaCl_3$ and the corresponding chlorides (see Scheme 1). For $[\mathbf{4}][GaCl_4]$, high-quality single crystals were obtained by crystallization from 1,2-dichloroethane. Its XRD structure is presented in Figure 1e.

dx.doi.org/10.1021/ic302203t | Inorg. Chem. 2013, 52, 3699−3710

Scheme 1. Preparation of the Salts

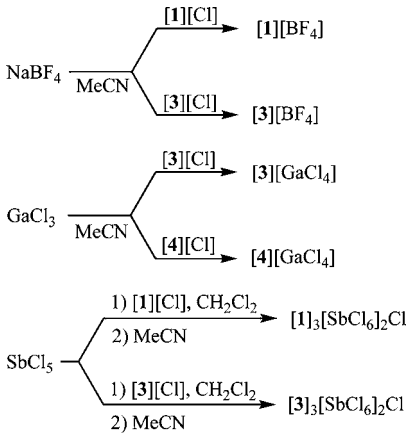

[3][$GaCl_4$] did not produce crystals suitable for XRD, whereas [1][$GaCl_4$] and [2][$GaCl_4$] were synthesized and structurally characterized previously.[1a]

In the salts [1][BF_4] and [3][BF_4], the cations form centrosymmetric dimers with short N···S contacts of 3.249(3) Å and 3.232(8) Å, respectively, which can be compared with the sum (3.35 Å) of the van der Waals (VdW) radii of N and S.[26] At the same time, there are no short contacts between the BF_4^- anions (Figure S1 in the Supporting Information). A similar formation of dimers by cations was previously observed for the tetrachlorogallates of 3*H*-naphtho[1,2-d][1,2,3]diselenazolium[8] and 1,2,3-benzothiatellurazolium.[1a] In contrast to those salts, there are no short contacts between the cations in [4][$GaCl_4$], but there are short contacts between the anions (Figure S1 in the Supporting Information), particularly Cl···Cl contacts with a distance of 3.4416(7) Å (the sum of VdW radii is 3.50 Å).[26]

Geometries and Electronic Structures of the Cations. According to the XRD data, the cations of salts [1][$GaCl_4$],[1a] [1][BF_4], [2][$GaCl_4$],[1a] [3][BF_4], and [4][$GaCl_4$] are planar to within 0.008, 0.113, 0.024, 0.070, and 0.072 Å, respectively. The experimental geometries of cation **1** in salts [1][BF_4] and [1][$GaCl_4$] display only minor differences which reflects the structural rigidity of the cation. The only exception is the C5C6 distance, but the reason for this is unclear. The geometry of **1** was optimized using MP2 and DFT methods. Taking into account the results of previous calculations on related sulfur–nitrogen heterocycles,[9] the following combinations of DFT functional and basis set were chosen: B1B95/6-311++G(d,p), B1B95/cc-pVTZ, B1B95/cc-pVQZ, and B3LYP/cc-pVTZ. MP2 was combined with the 6-311G(d,p) and cc-pVTZ basis sets. The B1B95/cc-pVQZ results have been presented in Table 3, while the results of the remaining methods have been gathered in Table S1 in the Supporting Information. Comparison of the results of the B1B95/cc-pVQZ calculations on **1** and the XRD data for [1][BF_4] and [1][$GaCl_4$] reveals that the trends in the bonds lengths are reproduced well. This overall agreement is also seen for the other method/basis set combinations in Table S1 in the Supporting Information, even though the absolute values of the parameters deviate more from the experimental ones for DFT/B3LYP and MP2 than they do for DFT/B1B95. Consequently, further calculations on **1**–**4** and **1**$^{\bullet}$–**4**$^{\bullet}$ were carried out using only B1B95/cc-pVQZ. The B1B95/cc-pVTZ combination will be used only for the calculations on the radical dimers, because of its lower computational cost. The cc-pVTZ basis set was also used for the GIAO NMR chemical shift calculations for **1**–**4**, because it produces better results than cc-pVQZ.

Table 3 also contains the calculated Hirshfeld bond orders for cations **1**–**4** and the related 1,3,2-benzodithiazolium cation (**5**), which provide more insight into the bonding. For all cations, the bonds have lengths intermediate between the typical values for single and double bonds.[26b,27] For **1**, the bond orders vary between 1.21 and 1.70. Despite the fact that the S–S bond is only slightly shorter than a typical S–S single bond (~2.070 Å), its bond order in **1** is substantially higher than 1. Replacement of S by Se leads to a decrease of the bond orders of the involved bonds, but it has practically no effect on the other bond orders. The carbocycles of **1**–**4** have ortho-quinoid character as the C4C5 and C6C7 bond distances/bond orders are shorter/higher, compared with the other CC bonds. To a lesser extent, the same is true for cation **5**.[28]

Table 4 displays the Hirshfeld charge distributions for cations **1**–**5** obtained from the B1B95/cc-pVQZ calculations. In **1**–**4**, the positive charge is mainly localized on the heterocycle, more precisely on the two chalcogen atoms. Atoms C3a and C6 of all cations, and also atom C7a of cations **1** and **2**, bear significant positive charges. The charge distribution in the carbocycle is very important for the reactivity of the cations under discussion: in particular, nucleophilic substitutions are known to proceed usually at C6,[1c,24a] which seems to be consistent with the calculated charges. The N atom is charged negatively. Replacement of S by Se significantly affects only the adjacent atoms. The symmetrical isomer of **1**, cation **5**, features less delocalization of the positive charge onto the carbocycle.

Solution NMR Data and NICS Values for the Cations. Multinuclear NMR data for cations **1**–**5**, both experimental (in solution) and calculated, are presented in Table 5. Both the cc-pVTZ and cc-pVQZ basis sets were used for the chemical shift calculations. The former (Table 5) yielded better results than the latter (see Table S2 in the Supporting Information) in all cases except for C3a in **3** and **4**. For the ^{14}N NMR spectra, the linewidths are large (1200 Hz for [4][$GaCl_4$] in CD_3CN). Assignment of the experimental data is mainly tentative and based on the results of the calculations; for ^{1}H NMR also, the multiplicity of the signals is used.

According to the calculations, the most downfield signal in the ^{13}C NMR spectra of **1** and **2** belongs to C3a, and the next to C7a, whereas for **3** and **4** this sequence is reversed. This is in contrast with the experimental data obtained for [4][$GaCl_4$], for which the signal of C7a can be unambiguously identified via ^{13}C–^{77}Se coupling. It can be assumed that, in the case of **3** and **4**, the calculated chemical shift of C7a is overestimated and the most downfield signal corresponds to C3a.

As a whole, the experimental chemical shifts are satisfactorily reproduced by the calculations. The best agreement is observed for δ^1H and δ^{13}C. Calculated δ^1H, δ^{13}C, and $\delta^{15(14)}$N are, in most cases, overestimated, whereas the δ^{77}Se are underestimated.

For **1**–**4**, the effects of the solvent (CD_3CN vs CF_3COOH) and the anion (Cl^-, BF_4^-, or $GaCl_4^-$) on the chemical shifts are minor and usually do not exceed 2%. The largest difference (4%) is observed for the nitrogen spectra of **1** (see Table 5).

The difference between the calculated ^{33}S chemical shifts for the two S atoms of **1** (not determined experimentally)[30] is only 40–50 ppm. Taking into account the linewidths in the ^{33}S NMR spectra of related thiazoles and isothiazoles (4200 and 7700 Hz, respectively)[31] one can conclude that the experimental signals cannot be resolved with conventional techniques.

dx.doi.org/10.1021/ic302203t | *Inorg. Chem.* 2013, 52, 3699–3710

Table 3. Bond Lengths and Bond Orders of Cations 1−5[a]

Cation 1, Salts [1][BF_4] and [1][$GaCl_4$][b]				
	Bond Length, According to XRD [Å]		B1B95/cc-pVQZ	
bond	1, [BF_4]	1, [$GaCl_4$]	length (Å)	order
C3aN3	1.341(4)	1.345(4)	1.327	1.54
S1S2	2.028(1)	2.024(1)	2.034	1.21
S2N3	1.577(3)	1.561(3)	1.565	1.70
C7aCh1	1.698(3)	1.693(3)	1.699	1.33
C3aC7a	1.428(4)	1.437(4)	1.434	1.23
C3aC4	1.422(4)	1.407(4)	1.412	1.37
C4C5	1.362(4)	1.352(5)	1.360	1.64
C5C6	1.413(5)	1.383(5)	1.412	1.40
C6C7	1.372(4)	1.357(5)	1.372	1.58
C7C7a	1.409(4)	1.397(4)	1.393	1.47

Cation 2, Salt [2][$GaCl_4$][b]			
		B1B95/cc-pVQZ	
bond	bond length, according to XRD (Å)	length (Å)	order
C3aN3	1.324(5)	1.320	1.60
S1Se2	2.174(1)	2.168	1.13
Se2N3	1.740(3)	1.721	1.44
C7aS1	1.711(4)	1.699	1.34
C3aC7a	1.422(4)	1.439	1.22
C3aC4	1.430(5)	1.419	1.34
C4C5	1.344(5)	1.357	1.65
C5C6	1.405(6)	1.412	1.40
C6C7	1.358(6)	1.371	1.59
C7C7a	1.391(5)	1.394	1.46

Cation 3, Salt [3][BF_4]			
		B1B95/cc-pVQZ	
bond	bond length, according to XRD (Å)	length (Å)	order
C3aN3	1.334(1)	1.327	1.55
Se1S2	2.162(3)	2.175	1.11
S2N3	1.587(9)	1.564	1.72
C7aSe1	1.840(9)	1.842	1.17
C3aC7a	1.424(1)	1.431	1.26
C3aC4	1.395(2)	1.414	1.36
C4C5	1.383(2)	1.360	1.64
C5C6	1.419(2)	1.409	1.42
C6C7	1.347(2)	1.374	1.57
C7C7a	1.424(1)	1.390	1.49

Cation 4, Salt [4][$GaCl_4$]			
		B1B95/cc-pVQZ	
bond	bond length, according to XRD (Å)	length (Å)	order
C3aN3	1.330(3)	1.321	1.60
Se1Se2	2.2902(3)	2.296	1.08
Se2N3	1.742(2)	1.719	1.45
C7aSe1	1.850(2)	1.843	1.18
C3aC7a	1.435(3)	1.437	1.25
C3aC4	1.433(3)	1.421	1.33
C4C5	1.354(3)	1.358	1.65
C5C6	1.414(3)	1.409	1.42
C6C7	1.367(3)	1.373	1.58
C7C7a	1.396(3)	1.391	1.49

Cation 5, Salt [5][Cl][c]			
		B1B95/cc-pVQZ	
bond	bond length, according to XRD (Å)	length (Å)	order
C7aS1	1.714(4)	1.708	1.28
C3aS3	1.712(4)	1.708	1.28
N2S1	1.593(4)	1.587	1.60
N2S3	1.625(4)	1.587	1.60
C3aC7a	1.410(5)	1.409	1.33
C3aC4	1.413(5)	1.396	1.46
C4C5	1.370(5)	1.370	1.59
C5C6	1.411(5)	1.405	1.43
C6C7	1.366(6)	1.370	1.59
C7C7a	1.404(5)	1.396	1.46

[a]Numbering of atoms as shown in Chart 1. [b]Data taken from ref 1a. [c]Data taken from ref 28.

The Nucleus-Independent Chemical Shift (NICS)[29] values calculated for **1**−**4** and **5** at the B3LYP/cc-pVTZ//B1B95/cc-pVTZ level of theory are negative (see Table 6), clearly indicating the aromaticity of both the carbocycles and heterocycles of the cations. Replacement of S by Se only leads to a slight decrease of the NICS absolute values of the heterocycle. The NICS of the carbocycle decreases only with the replacement of S2 (cations **2** and **4**). It is interesting to note that cations **2** and **4** are more reactive toward nucleophilic substitution at C6:[24a] the reduction of the aromaticity could be used as the explanation for the decrease of the activation energy for the substitution. Transformation of **1** into **5** affects the aromaticity of both the heterocycles and carbocycles, as the carbocycle becomes more aromatic and the heterocycle becomes slightly less aromatic. Overall, cations **1**−**5** can be classified as 10π-electron heteroaromatics.

2.2. Herz Radicals. *Generation and EPR Characterization.* Radicals **1**$^{\bullet}$−**4**$^{\bullet}$ were obtained in toluene and CH_2Cl_2 solutions by the chemical reduction of the salts of the corresponding cations with Ph_3Sb and characterized by EPR spectroscopy (Figure 2). The EPR spectra of **3**$^{\bullet}$ and **4**$^{\bullet}$ generated several times from independently prepared precursors were unresolved and determination of hfc constants was impossible in all cases. It is somewhat unexpected because reported spectra of naphtho analogues of the radicals studied are resolved enough to extract a_N constants.[8] Concentration dependence of the linewidths was not found for the spectra of **3**$^{\bullet}$ and **4**$^{\bullet}$ in the range of 1.0−0.1 mM. One may think that the line broadening observed is mostly caused by spin−orbit coupling at the Se atoms and large anisotropy of *g*-tensors of the radicals.[3c] The *g*-values measured for **3**$^{\bullet}$ and **4**$^{\bullet}$ were 2.01627 and 2.02433, respectively. A reason for the larger line broadening in the spectrum of **3**$^{\bullet}$, compared to that of **2**$^{\bullet}$ (Figure 2), is not entirely clear (spin−orbit coupling should be stronger for **2**$^{\bullet}$ than for **3**$^{\bullet}$, because of the larger spin density at the Se atom), although similar situation was observed previously for related tricyclic radicals.[5h]

Previous DFT calculations of the hfc constants for **1**$^{\bullet}$ with the B3LYP and B1B95 functionals revealed that the B1B95 functional, in combination with large basis sets such as cc-pVTZ and cc-pVQZ, produces better results for a_H but performs worse for a_N, compared with the smaller basis sets cc-pVDZ and 6-31G(d).[1a,3c,i,32] In this work, several other approaches were also used: the results of B3LYP/6-31G(d), B1B95/6-31G(d), B1B95/cc-pVDZ, B1B95/cc-pVTZ, and B1B95/cc-pVQZ calculations can be found in

dx.doi.org/10.1021/ic302203t | Inorg. Chem. 2013, 52, 3699−3710

Table 4. B1B95/cc-pVQZ Hirshfeld Atomic Charges in Cations 1−5

atom	1	2	3	4	5
C5	0.012	0.009	0.009	0.006	0.020
C6	0.037	0.037	0.036	0.035	0.020
C7	−0.012	−0.015	−0.015	−0.018	−0.005
C7a	0.024	0.024	0.006	0.007	0.004
C3a	0.069	0.066	0.064	0.062	0.004
C4	0.008	0.007	0.008	0.007	−0.005
Ch1	0.233	0.197	0.302	0.267	0.350
Ch2	0.341	0.418	0.309	0.384	0.350
N3	−0.052	−0.077	−0.052	−0.079	−0.074
H4	0.088	0.085	0.086	0.084	0.082
H5	0.084	0.083	0.083	0.082	0.085
H6	0.087	0.086	0.086	0.085	0.085
H7	0.082	0.080	0.079	0.077	0.082
carbocycle	0.477	0.462	0.441	0.428	0.373
heterocycle	0.615	0.628	0.629	0.641	0.634

Table 7, together with the experimental data. The results of MP2/6-311G(d,p), MP2/cc-pVTZ, PBE/cc-pVDZ, PBE/cc-pVTZ, PBE0/cc-pVDZ, PBE0/cc-pVTZ, B3LYP/cc-pVDZ, B3LYP/cc-pVTZ, B3LYP/cc-pVQZ, B1B95/aug-cc-pVDZ, B1B95/aug-cc-pVTZ and B1B95/aug-cc-pVQZ calculations for the radical **1**$^{\bullet}$ as well as B3LYP and B1B95 a_C constants can be found in Tables S3 and S4 in the Supporting Information. It was found that the PBE functional underestimates all hfc constants. The MP2 method underestimates a_N and strongly overestimates a_H constants. The a_S constants[1g] are satisfactorily reproduced by the B1B95 functional with the cc-pVDZ, cc-pVQZ, and aug-cc-pVQZ basis sets, as well as by PBE0/cc-pVTZ and B3LYP/cc-pVTZ (see Table 7 and Table S3 in the Supporting Information). The experimental and calculated data for **1**$^{\bullet}$**−4**$^{\bullet}$ suggest that replacement of S by Se results in only minor changes of both the experimental and calculated hfc constants.

For radical **5**$^{\bullet}$, the EPR spectrum consists of a 1:1:1 triplet featuring practically no hyperfine splitting due to spin coupling with the protons. Most of the spin density is localized on the heterocycle. Measured (B3LYP/cc-pVDZ calculated) hfc constants are a_N = 11.4 (10.5) and a_H = 0.5 (−0.4), 0.5 (−0.2) G.[3i]

Table 6. Nucleus-Independent Chemical Shift (NICS) Values[a] for Cations 1−5 at the B3LYP/cc-pVTZ Level for B1B95/cc-pVTZ Geometries

	Chemical Shift			
	Carbocycle		Heterocycle	
cation	NICS(0)	NICS(1)	NICS(0)	NICS(1)
1	−6.49	−9.65	−15.39	−12.81
2	−5.77	−9.10	−14.34	−12.27
3	−6.56	−9.61	−14.72	−12.39
4	−5.46	−9.00	−14.82	−12.56
5	−10.42	−12.04	−13.26	−11.87

[a]The NICS(0) and NICS(1) notations denote the values at the center of the cycle and at a point 1 Å above the center of cycle, respectively.

Geometries and Electronic Structures. Calculated (B1B95/cc-pVQZ) bond lengths and bond orders for radicals **1**$^{\bullet}$**−4**$^{\bullet}$ are presented in Table 8; the corresponding B1B95/cc-pVTZ values are given in Table S5 in the Supporting Information. Addition of an electron to cations **1−4** leads to the occupation of an antibonding π^*-orbital. Consequently, it results in the elongation of the C3a−N3 bonds by 0.017−0.023 Å, the Ch1−Ch2 bonds by 0.045−0.053 Å, the Ch2−N3 bonds by 0.044−0.045 Å, and the C7a−Ch1 bonds by 0.036−0.039 Å, and in the shortening of the C3a−C7a bond by 0.014−0.019 Å. At the same time, the short bonds of the carbocycle are elongated (C4−C5 by 0.011−0.013 Å and C6−C7 by 0.070−0.090 Å), whereas the long ones are shortened (C3a−C4 and C7−C7a by 0.050−0.090 Å, and C5−C6 by 0.015−0.018 Å). Thus, the transformation of cations **1−4** into radicals **1**$^{\bullet}$**−4**$^{\bullet}$ leads to an increase in the bond lengths and an associated decrease in the bond orders for the bonds between the chalcogen and N atoms, and to an equalization of the CC bonds (see Table 8). This is in agreement with the antibonding character of π^*-SOMO.

Table 5. Experimental and Calculated (GIAO, B3LYP/cc-pVTZ Values) Multinuclear NMR Data for Cations 1−4 and 5

	^{13}C NMR, δ [ppm]						^{33}S or ^{77}Se NMR, δ [ppm]		^{15}N NMR, δ [ppm]	^{1}H NMR, δ [ppm]			
cation	C5	C6	C7	C7a	C3a	C4	Ch1	Ch2	N3	H4	H5	H6	H7
1 GIAO	141.9	151.8	127.8	162.2	166.2	138.2	143.5	187.3	465.2	9.48	8.90	9.08	9.05
1[Cl][a, 2]	133.9	139.1	123.4	156.2	164.0	128.1			406[b]	9.09	8.46	8.65	9.00
1[BF_4]	135.2	139.6	125.6	158.2	165.9	129.5			403.2	8.85	8.24	8.42	8.84
1[$GaCl_4$]	134.6	139.3	124.9	157.0	164.9	129.0			388.7	8.86	8.27	8.45	8.83
2 GIAO	140.5	152.4	128.9	166.3	168.8	138.1	131.3	1363	512.9	9.32	8.82	9.03	9.05
2[$GaCl_4$]	133.8	139.4	127.4	162.2	169.9	130.7		1556		8.69	8.08	8.40	8.66
3 GIAO	140.7	150.0	129.8	172.9	166.9	141.2	1267	224.3	491.4	9.66	8.85	8.95	9.14
3[Cl][c]	132.2	139.0	128.9	167.1	170.3	135.1	1410		425[b]	9.17	8.22	8.43	9.02
3[$GaCl_4$]	131.2	137.7	128.6	166.0	169.7	134.3	1423		421[b]	9.08	8.18	8.37	8.84
4 GIAO	139.4	150.1	130.7	177.2	169.4	140.6	1207	1392	532.5	9.50	8.79	8.89	9.18
4[Cl][c]	132.2	137.1	129.8	169.1	173.8	133.2	1344	1581	459.3	8.94	7.94	8.36	8.78
4[$GaCl_4$]	131.8	137.0	130.2	168.7[d]	173.6	133.3	1350[e]	1601[e]	454.3	8.93	7.95	8.37	8.68
5 GIAO	141.4	141.4	128.1	169.9	169.9	128.1	228.1	228.1	441.2	9.33	8.83	8.83	9.33
5[Cl][a, 2]	132.6	132.6	122.8	163.3	163.3	122.8			378[b]	9.09	8.22	8.22	9.09

[a]In CF_3COOH. [b]^{14}N NMR. [c]In $CF_3COOH/CDCl_3$ 4:1. [d]$J(^{13}C-^{77}Se)$ = 152 Hz. [e]$J(^{77}Se-^{77}Se)$ = 356 Hz.

dx.doi.org/10.1021/ic302203t | Inorg. Chem. 2013, 52, 3699−3710

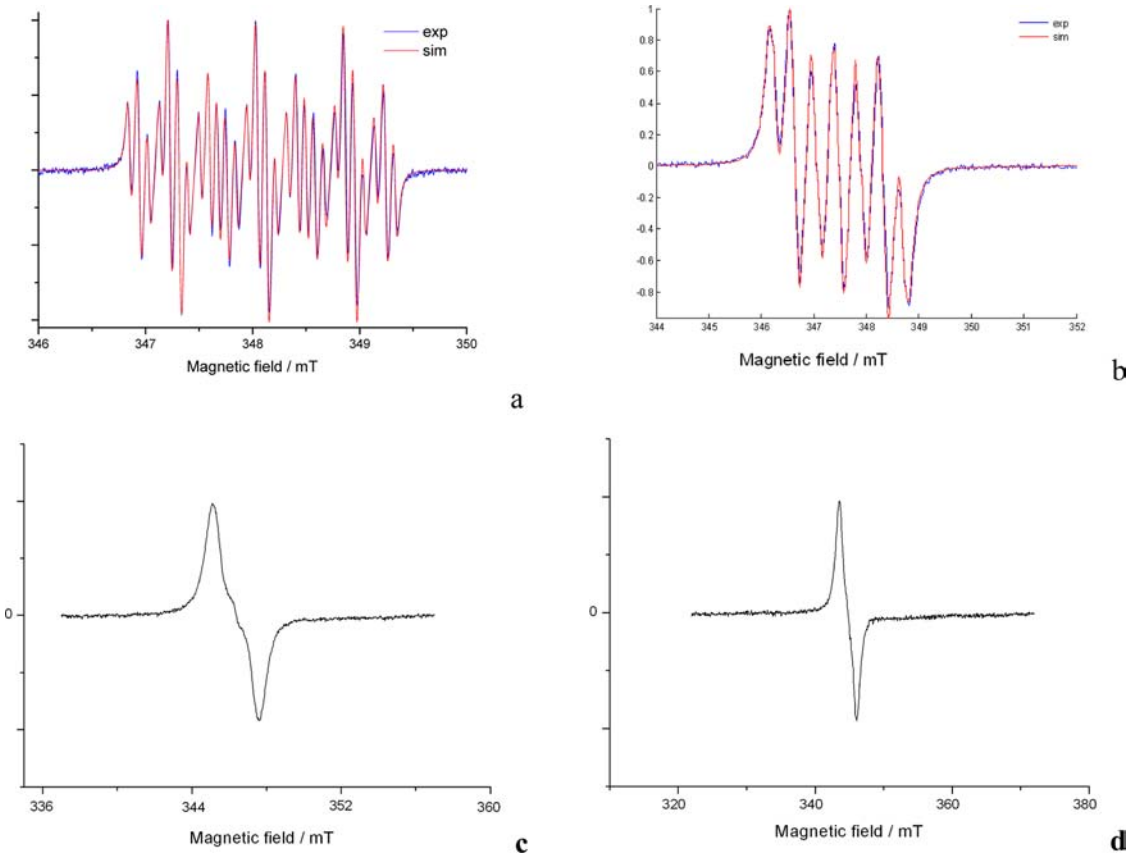

Figure 2. Experimental (exp) EPR spectra of radicals (a) **1**•, (b) **2**•, (c) **3**•, and (d) **4**• and the associated simulations (sim) for **1**• and **2**•.

The addition of an electron to cations **1**−**4** results, as expected, in a reduction of the charges on all atoms (see Table 9). The largest changes are observed for the N and chalcogen atoms, namely, a decrease of 0.196−0.264. Among the C atoms, C6 displays the largest decrease (0.079−0.081), while the values for C4 and C5 (0.048−0.052), C7a (0.041−0.045), and C3a and C7 (0.031−0.038) are smaller. The same trends are observed for the H atoms: 0.038−0.040 for H6, 0.034−0.036 for H4 and H5, and 0.029−0.032 for H7. In total, the charge changes by 0.416−0.453 for the carbocycle and by 0.638−0.659 for the heterocycle (note that the sum is not equal to 1, since C3a and C7a are common to both cycles). As a result, in the radicals the N atoms bear the largest negative charges; the chalcogen atoms are positive and the charges are, as expected, larger for the atoms in the 2-positions than for those in the 1-positions (see Table 9). The C atoms are charged negatively, excluding C3a. The absolute values of the charges of atoms C4−C7 are close to those of the positively charged H atoms attached to them. Thus, both the carbocycles and the heterocycles have small total charges. In contrast to cations **1**−**4**, the charge distribution in the radicals seems to be determined mainly by the inductive effects of the atoms.

The spin densities in **1**•−**4**• are mainly localized on the heteroatoms, especially on the N atom (Table 10). Only 22%−24% of the spin density is transferred onto the carbocycle, and then mainly to C4, C6, and C7a. This pattern resembles the spin-density distribution in the benzyl radical.[3i,33] Replacement of S by Se does not affect the spin-density distribution to any great extent (cf. refs 1a and 8).

The Radical Dimers. 1,2,3-Dithiazolyls, monomeric in solution, reveal a general propensity for dimerization in the solid state, which is very important for their macroscopic magnetic and electrical properties.[4−8,34] The same is true for 1,3,2-dithiazolyls.[28b] According to the XRD data, in the dimers the radicals are coplanar and connected by very long and weak S···S interactions.[4−8,28b,34] There are no data on the dimerization of Se-containing monocyclic or benzo-fused 1,2,3-dichalcogenazolyls. For tricyclic pyrido- and pyrazino-bis[1,2,3]-dichalcogenazolyls, the dimerization features the formation of C−C, S−S, and Se−Se covalent bonds.[5] In all cases, the solid-state dimerization is reversible and in solution the dimers dissociate, which indicates that their constituent monomers are weakly bonded. Previously reported gas-phase calculations for several 1,3,2-dithiazolyls, and 1,2,3,5- and 1,3,2,4-dithiadiazolyls, predicted low (<10 kcal mol^{-1}) or even zero dimerization energies.[7]

In this work, the radical dimers $[\mathbf{1}^{\bullet}]_2$−$[\mathbf{4}^{\bullet}]_2$ were calculated using the B1B95/cc-pVTZ method in seven different configurations with short contacts between different pairs of heteroatoms, and with stacked or lateral geometries (see Figure S2 in the Supporting Information): the short contacts and types of configurations are Ch1···Ch1′ and Ch2···Ch2′, stacked (*a*) and lateral (*b*); Ch1···Ch2′ and Ch2···Ch1′, lateral (*c*) and stacked (*d*); N···Ch′ and Ch···N′, lateral (*e*) and stacked (*f*); Ch···Ch′ and N···N′, lateral (*g*).

It was found that the dimerization energies are positive (i.e., the dimers are thermodynamically unstable; see Table 11), and that the intermolecular Hirshfeld bond orders are negative in practically all cases (see Tables S6−S9 in the Supporting Information); negative bond orders, arising from the scaling procedure,[10] indicate that bonding between the radicals in dimers is very weak. The only exception is lateral dimer $[\mathbf{2}^{\bullet}]_2$ in configuration *e* with N···Se contacts ($[\mathbf{2}^{\bullet}]_2e$; see Figure 3),

dx.doi.org/10.1021/ic302203t | *Inorg. Chem.* 2013, 52, 3699−3710

Table 7. Experimental and Calculated EPR Data for Radicals $1^{\bullet}$–$4^{\bullet}$

	hfc Constants [mT]					
		B3LYP	B1B95			
atom	exp	6-31G(d)	6-31G(d)	cc-pVDZ	cc-pVTZ	cc-pVQZ
			Radical $1^{\bullet}$[a]			
S1	0.355[b]	0.191	0.276	0.335	0.380	0.341
S2	0.451[b]	0.214	0.364	0.463	0.532	0.450
N3	0.819	0.885	0.884	1.002	0.464	0.491
H4	0.290	−0.409	−0.372	−0.327	−0.310	−0.306
H5	0.080	0.167	0.131	0.111	0.102	0.096
H6	0.369	−0.463	−0.420	−0.374	−0.363	−0.357
H7	0.097	0.172	0.134	0.112	0.103	0.098
			Radical $2^{\bullet}$			
S1		0.199	0.283	0.336	0.380	0.341
N3	0.838	0.851	0.859	1.002	0.464	0.495
H4	0.307	−0.409	−0.371	−0.328	−0.314	−0.312
H5	0.107	0.170	0.134	0.116	0.109	0.105
H6	0.391	−0.470	−0.424	−0.383	−0.377	−0.374
H7	0.107	0.179	0.139	0.120	0.115	0.111
			Radical $3^{\bullet}$[a]			
S2		0.213	0.359	0.444	0.506	0.424
N3	0.928	0.880	0.878	1.003	0.469	0.497
H4	0.303	−0.414	−0.378	−0.333	−0.317	−0.314
H5	0.089	0.175	0.139	0.121	0.114	0.109
H6	0.350	−0.467	−0.424	−0.381	−0.371	−0.365
H7	0.103	0.177	0.140	0.121	0.115	0.110
			Radical $4^{\bullet}$[a]			
N3	0.974	0.839	0.845	0.997	0.466	0.497
H4	0.296	−0.412	−0.373	−0.333	−0.319	−0.318
H5	0.100	0.176	0.139	0.124	0.119	0.115
H6	0.393	−0.471	−0.425	−0.388	−0.383	−0.380
H7	0.111	0.181	0.143	0.127	0.123	0.120

[a]The experimental and B1B95 data for a_H and a_N are taken from ref 3c. [b]For 5,7-di-*tert*-butyl-1,2,3-benzodithiazolyl; for 4,6-di-*tert*-butyl-1,2,3-benzodithiazolyl, a_S = 0.369 and 0.451 mT.[1g]

which is 13.6 kJ mol^{-1} more stable than the system of two noninteracting radicals $2^{\bullet}$.

For dimer $[2^{\bullet}]_2e$, the N···Se distance is 2.044 Å, which corresponds to a Hirshfeld bond order of 0.46. The S–Se bonds of the components of $[2^{\bullet}]_2e$ are elongated (2.350 Å) and weaker (Hirshfeld bond order 0.81) than the S–Se bonds of the isolated radical $2^{\bullet}$ (2.216 Å and 1.13, respectively). The dimerization of $2^{\bullet}$ also leads to the elongation and weakening of the N–Se bonds: the bond lengths and bond orders, respectively, are 1.801 Å and 1.03 for $[2^{\bullet}]_2e$ and 1.769 Å and 1.31 for $2^{\bullet}$. On the other hand, the C–S bonds becomes shorter and stronger: the bond lengths and bond orders are, respectively, 1.723 Å and 1.41 in $[2^{\bullet}]_2e$, and 1.742 Å and 1.31 in $2^{\bullet}$).

Among dimers $[1^{\bullet}]_2e$, $[2^{\bullet}]_2e$, and $[3^{\bullet}]_2e$, stronger N···Ch2 interactions are observed for radicals with larger charges at

Table 9. Atomic Charges in Radicals $1^{\bullet}$–$4^{\bullet}$ (B1B95/cc-pVQZ)

	Atomic Charge			
atom	$1^{\bullet}$	$2^{\bullet}$	$3^{\bullet}$	$4^{\bullet}$
C5	−0.040	−0.042	−0.041	−0.042
C6	−0.044	−0.044	−0.044	−0.044
C7	−0.047	−0.048	−0.048	−0.049
C7a	−0.021	−0.021	−0.034	−0.034
C3a	0.031	0.028	0.031	0.028
C4	−0.043	−0.043	−0.042	−0.042
Ch1	0.024	0.001	0.058	0.037
Ch2	0.105	0.152	0.083	0.127
N3	−0.162	−0.178	−0.158	−0.176
H4	0.052	0.051	0.052	0.050
H5	0.049	0.048	0.048	0.048
H6	0.047	0.047	0.047	0.047
H7	0.050	0.049	0.049	0.048
carbocycle	0.034	0.026	0.017	0.012
heterocycle	−0.023	0.018	−0.020	−0.018

Table 10. Spin Densities in $1^{\bullet}$–$4^{\bullet}$ (B1B95/cc-pVQZ)

	Spin Density			
atom	$1^{\bullet}$	$2^{\bullet}$	$3^{\bullet}$	$4^{\bullet}$
C5	−0.013	−0.015	−0.016	−0.017
C6	0.095	0.100	0.097	0.101
C7	−0.015	−0.018	−0.017	−0.020
C7a	0.084	0.093	0.088	0.096
C3a	−0.006	−0.005	−0.009	−0.007
C4	0.080	0.082	0.082	0.083
Ch1	0.148	0.142	0.149	0.144
Ch2	0.287	0.265	0.289	0.266
N3	0.331	0.349	0.330	0.345
H4	0.004	0.004	0.004	0.004
H5	−0,001	−0.001	−0.001	−0.002
H6	0.007	0.007	0.007	0.007
H7	−0.002	−0.002	−0.002	−0.002
carbocycle	0.233	0.244	0.233	0.246
heterocycle	0.843	0.844	0.848	0.844

Table 8. B1B95/cc-pVQZ Bond Lengths and Bond Orders in Radicals $1^{\bullet}$–$4^{\bullet}$

	$1^{\bullet}$		$2^{\bullet}$		$3^{\bullet}$		$4^{\bullet}$	
bond	length [Å]	order	length [Å]	order	length [Å]	order	length [Å]	order
C3aN3	1.346	1.51	1.343	1.55	1.344	1.52	1.341	1.56
Ch1Ch2	2.087	1.11	2.213	1.05	2.226	1.02	2.342	1.01
Ch2N3	1.610	1.58	1.766	1.33	1.608	1.60	1.764	1.35
C7aCh1	1.737	1.24	1.738	1.24	1.878	1.09	1.881	1.09
C3aC7a	1.417	1.32	1.420	1.32	1.417	1.34	1.419	1.34
C3aC4	1.404	1.43	1.410	1.40	1.407	1.41	1.413	1.39
C4C5	1.373	1.61	1.370	1.62	1.372	1.61	1.369	1.63
C5C6	1.394	1.51	1.395	1.51	1.393	1.51	1.394	1.51
C6C7	1.381	1.57	1.379	1.58	1.381	1.57	1.380	1.57
C7C7a	1.385	1.53	1.388	1.51	1.384	1.54	1.386	1.53

dx.doi.org/10.1021/ic302203t | Inorg. Chem. 2013, 52, 3699–3710

Table 11. Dimerization Energies for the Dimers of Radicals 1•−4• (B1B95/cc-pVTZ)

	Dimerization Energy [kJ mol^{-1}]						
dimer	configuration a	configuration b	configuration c	configuration d	configuration e	configuration f	configuration g
$[\mathbf{1}^{\bullet}]_2$	26.3	80.8	80.7	38.0	57.1	22.3	86.3
$[\mathbf{2}^{\bullet}]_2$	22.6	76.6	73.9	35.1	−13.6	19.5	79.4
$[\mathbf{3}^{\bullet}]_2$	24.3	78.5	77.0	33.0	55.7	20.6	85.2
$[\mathbf{4}^{\bullet}]_2$	17.7	73.1	64.9	32.4	78.7	12.4	76.5

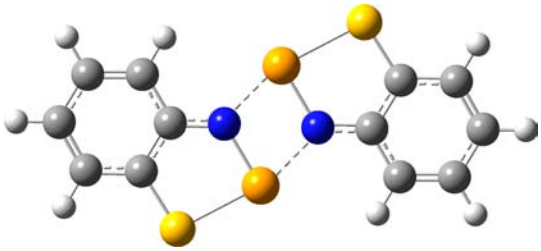

Figure 3. Optimized structure of the lateral dimer $[\mathbf{2}^{\bullet}]_2e$ with contacts Se2···N and N···Se2. Color code: gray = C, light gray = H, blue = N, yellow = S, orange = Se.

these atoms. At the same time, dimer $[\mathbf{4}^{\bullet}]_2e$ having, similar to $[\mathbf{2}^{\bullet}]_2e$, N···Se contacts in combination with considerable charges on the N and Se atoms, is unstable, and a general correlation between the charges on the interacting atoms and the energies of dimerization seems to be absent.

Importantly, a similar mode of dimerization is also observed for many 1,2,3-dichalcogenazolium salts, namely, [**1**][BF_4] and [**3**][BF_4] (present work), and 3*H*-naphtho[1,2-d][1,2,3]diselenazolium and 1,2,3-benzothiatellurazolium tetrachlorogallates.[1a,8]

For the dimers of the other studied types, the Ch2···Ch2 interactions are stronger than Ch1···Ch1 (*a*-, *b*-, and *g*-type interactions) or Ch1···Ch2 (*c* and *d* types), or N···Ch2 (*f*-type) interactions. Bonding between the N atoms is almost absent in the *a*- and *g*-type interactions. Except for $[\mathbf{2}^{\bullet}]_2e$, the stacked dimers are 40−65 kJ mol^{-1} more stable than the lateral ones, probably because of many weak bonding interactions resembling π-stacking interactions.

Overall, radicals **1**•−**4**• have no inherent tendency toward dimerization in the free state, and the observed solid-state dimerization of chalcogen-nitrogen heterocyclic π-radicals[4−8] seems to be driven by packing forces.

4. CONCLUSIONS

A combined experimental and computational study on the structure and properties of the archetypal Herz cations and radicals and their Se congeners was performed. The B1B95/cc-pVQZ method was found to reproduce the trends in the experimentally determined bonds lengths well. More time-economic B1B95/cc-pVTZ calculations provide similar results and can also be used in computational studies of 1,2,3-benzodithiazolium and its Se congeners.

The calculations on the cations reveal a delocalization of the positive charge over both the heterocycles and the carbocycles. Hirshfeld bond orders of the bonds in both rings lie between 1 and 2, indicating cyclic π-conjugation. According to the NICS values, 1,2,3-benzodichalcogenazoliums can be classified as 10 π-electron heteroaromatics.

Neutral π-radicals related to the cations, i.e., 1,2,3-benzodichalcogenazolyls, are also delocalized systems: the B1B95/cc-pVQZ calculations show a delocalization of ∼20% of the spin density onto their carbocycles.

Replacement of S by Se leads to a limited perturbation of the molecular and electronic structures of both cations and radicals, and notable changes are observed only at the involved and neighboring sites. At the same time, the EPR spectra of the Se-containing radicals reveal spin−orbit broadening of the spectral lines, especially for the radicals with the Se atom in the 1-position. This magnetic anisotropy is important in terms of the magnetic properties of the corresponding solids, which are targets of further work.

The B1B95/cc-pVTZ dimerization energies of the radicals in the gas phase were found to be generally positive, indicating that the dimers are unstable. A negative energy was observed in one case only, but its low value implies very weak bonding between the individual radicals. One can therefore assume that the previously reported solid-state dimerization of various chalcogen−nitrogen π-radicals, which affects their magnetic properties, is driven by the packing forces of the crystal lattices. Thus, one can expect that, with crystal engineering methods, it is possible to obtain solids composed of nondimerized (i.e., paramagnetic) 1,2,3-benzodichalcogenazolyls, as has been successfully done for their 1,3,2-isomers.

■ ASSOCIATED CONTENT

Supporting Information

This material is available free of charge via the Internet at http://pubs.acs.org.

■ AUTHOR INFORMATION

Corresponding Author

*E-mail addresses: makarov@nioch.nsc.ru (A.Yu.M.), frank.blockhuys@ua.ac.be (F.B.), zibarev@nioch.nsc.ru (A.V.Z.).

Notes

The authors declare no competing financial interest.

■ ACKNOWLEDGMENTS

The authors are grateful to Dr. Karla Tersago and Prof. Dr. Christian Van Alsenoy for their help with the quantum chemical calculations, and to Prof. Dr. Matvey V. Fedin and Dr. Irina G. Irtegova for the EPR measurements. A.Yu.M. and F.B. thank INTAS (Project No. 05-109-4637), and A.Yu.M. thanks the Russian Federal Agency on Science and Innovations (Grant of the President of Russian Federation, No. MK-3178.2005.3) and the Russian Science Support Foundation (postdoctoral scholarship) for financial support.

■ DEDICATION

Dedicated to Prof. Dr. Dr. H. C. Rüdiger Mews on the occasion of his 70th birthday.

■ REFERENCES

(1) (a) Risto, M.; Assoud, A.; Winter, S. M.; Oilunkaniemi, R.; Laitinen, R. S.; Oakley, R. T. *Inorg. Chem.* **2008**, *47*, 10100−10109. (b) Rawson, J. M.; MacManus, G. D. *Coord. Chem. Rev.* **1999**, *189*,

135−168. (c) Kirsch, G. In *Methoden der Organische Chemie (Houben-Weyl)*; Schaumann, E., Ed.; Georg Thieme: Stuttgart, Germany, 1994; Bd. *E8d*, pp 3−12. (d) Mayer, R. *Phosph. Sulf.* **1985**, *23*, 277−296. (e) Mayer, R.; Domschke, G.; Bleisch, S.; Fabian, J.; Bartl, A.; Stasko, A. *Collect. Czech. Chem. Commun.* **1984**, *49*, 684−703. (f) Tsveniashvili, V. S. *Collect. Czech. Chem. Commun.* **1982**, *47*, 203−209. (g) Mayer, R.; Domschke, G.; Bleisch, S.; Bartl, A.; Stasko, A. *Z. Chem.* **1981**, *21*, 264−265. (h) Schneller, S. *Int. J. Sulfur Chem.* **1976**, *8*, 579−597. (i) Warburton, W. K. *Chem. Rev.* **1957**, *57*, 1011−1020.

(2) (a) Makarov, A. Yu. Dissertation, Institute of Organic Chemistry, Russian Academy of Sciences, Novosibirsk, Russia, 2002. (b) Makarov, A. Yu.; Bagryanskaya, I. Yu.; Gatilov, Yu. V.; Mikhalina, T. V.; Shakirov, M. M.; Shchegoleva, L. N.; Zibarev, A. V. *Heteroatom Chem.* **2001**, *12*, 563−576.

(3) (a) Gritsan, N. P.; Makarov, A. Yu.; Zibarev, A. V. *Appl. Magn. Reson.* **2011**, *4*, 449−466. (b) Makarov, A. Yu.; Zhivonitko, V. V.; Makarov, A. G.; Zikirin, S. B.; Bagryanskaya, I. Yu.; Bagryansky, V. A.; Gatilov, Yu. V.; Irtegova, I. G.; Shakirov, M. M.; Zibarev, A. V. *Inorg. Chem.* **2011**, *50*, 3017−3027. (c) Pivtsov, A. V.; Kulik, L. N.; Makarov, A. Yu.; Blockhuys, F. *Phys. Chem. Chem. Phys.* **2011**, *13*, 3873−3880. (d) Gritsan, N. P.; Pritchina, E. A.; Bally, T.; Makarov, A. Yu.; Zibarev, A. V. *J. Phys. Chem. A* **2007**, *111*, 817−824. (e) Gritsan, N. P.; Kim, S. N.; Makarov, A. Yu.; Chesnokov, E. N.; Zibarev, A. V. *Photochem. Photobiol. Sci.* **2006**, *5*, 95−101. (f) Makarov, A. Yu.; Kim, S. N.; Gritsan, N. P.; Bagryanskaya, I. Yu.; Gatilov, Yu. V.; Zibarev, A. V. *Mendeleev Commun.* **2005**, *15*, 14−17. (g) Shuvaev, K. V.; Bagryansky, V. A.; Gritsan, N. P.; Makarov, A. Yu.; Molin, Yu. N.; Zibarev, A. V. *Mendeleev Commun.* **2003**, *13*, 178−178. (h) Gritsan, N. P.; Bagryansky, V. A.; Vlasyuk, I. V.; Molin, Yu. N.; Makarov, A. Yu.; Platz, M. S.; Zibarev, A. V. *Russ. Chem. Bull.* **2001**, *50*, 2064−2070. (i) Vlasyuk, I. V.; Bagryansky, V. A.; Gritsan, N. P.; Molin, Yu. N.; Makarov, A. Yu.; Gatilov, Yu. V.; Shcherbukhin, V. V.; Zibarev, A. V. *Phys. Chem. Chem. Phys.* **2001**, *3*, 409−415. (j) Bagryansky, V. A.; Vlasyuk, I. V.; Gatilov, Yu. V.; Makarov, A. Yu.; Molin, Yu. N.; Shcherbukhin, V. V.; Zibarev, A. V. *Mendeleev Commun.* **2000**, *10*, 5−7.

(4) (a) Ratera, I.; Veciana, J. *Chem. Soc. Rev.* **2012**, *41*, 303−349. (b) Heynes, D. A. *CrystEngComm* **2011**, *13*, 4793−4805. (c) *Stable Radicals: Fundamentals and Applied Aspects of Odd-Electron Compounds*; Hicks, R.G., Ed.; Wiley: New York, 2010.

(5) (a) Winter, S. M.; Datta, S.; Hill, S.; Oakley, R. T. *J. Am. Chem. Soc.* **2011**, *133*, 8126−8129. (b) Leitch, A. A.; Lekin, K.; Winter, S. M.; Downie, L. E.; Tsuruda, H.; Tse, J. S.; Mito, M.; Desgreniers, S.; Dube, P. A.; Zhang, S.; Liu, Q.; Jin, C.; Ohishi, Y.; Oakley, R. T. *J. Am. Chem. Soc.* **2011**, *133*, 6051−6060. (c) Tsuruda, H.; Mito, M.; Deguchi, H.; Takagi, S.; Leitch, A. A.; Lekin, K.; Winter, S. M.; Oakley, R. T. *Polyhedron* **2011**, *30*, 2997−3000. (d) Yu, X.; Mailman, A.; Dube, P. A.; Assoud, A.; Oakley, R. T. *Chem. Commun.* **2011**, *47*, 4655−4657. (e) Lekin, K.; Winter, S. M.; Downie, L. E.; Bao, X.; Tse, J. S.; Desgreniers, S.; Secco, R. A.; Dube, P. A.; Oakley, R. T. *J. Am. Chem. Soc.* **2010**, *132*, 16212−16224. (f) Tse, J. S.; Leitch, A. A.; Yu, X.; Bao, X.; Zhang, S.; Liu, Q.; Jin, C.; Secco, R. A.; Desgreniers, S.; Ohishi, Y.; Oakley, R. T. *J. Am. Chem. Soc.* **2010**, *132*, 4876−4886. (g) Leitch, A. A.; Yu, X.; Robertson, C. M.; Secco, R. A.; Tse, J. S.; Oakley, R. T. *Inorg. Chem.* **2009**, *48*, 9874−9882. (h) Robertson, C. M.; Leitch, A. A.; Cvrkalj, K.; Reed, R. W.; Myles, D. J. T.; Dube, P. A.; Oakley, R. T. *J. Am. Chem. Soc.* **2008**, *130*, 8414−8425. (i) Leitch, A. A.; Brusso, J. L.; Cvrkalj, K.; Reed, R. W.; Robertson, C. M.; Dube, P. A.; Oakley, R. T. *Chem. Commun.* **2007**, 3368−3370. (j) Leitch, A. A.; McKenzie, C. E.; Oakley, R. T.; Reed, R. W.; Richardson, J. F.; Sawyer, L. D. *Chem. Commun.* **2006**, 1088−1090. (k) Beer, L.; Brusso, J. L.; Haddon, R. C.; Itkis, M. E.; Kleinke, H.; Leitch, A. A.; Oakley, R. T.; Reed, R. W.; Richardson, J. F.; Secco, R. A.; Yu, X. *J. Am. Chem. Soc.* **2005**, *127*, 18159−18170. (l) Beer, L.; Brusso, J. L.; Haddon, R. C.; Itkis, M. E.; Leitch, A. A.; Oakley, R. T.; Reed, R. W.; Richardson, J. F. *Chem. Commun.* **2005**, 1543−1545. (m) Beer, L.; Cordes, A. W.; Haddon, R. C.; Itkis, M. E.; Oakley, R. T.; Reed, R. W.; Robertson, C. M. *Chem. Commun.* **2002**, 1872−1873. (n) Barclay, T. M.; Beer, L.; Cordes, A. W.; Oakley, R. T.; Preuss, K. E.; Taylor, N. J.; Reed, R. W. *Chem. Commun.* **1999**, 531−532. (o) Barclay, T. M.; Cordes, A. W.; Haddon, R. C.; Itkis, M. E.; Oakley, R. T.; Reed, R. W.; Zhang, H. *J. Am. Chem. Soc.* **1999**, *121*, 969−976.

(6) (a) Clarke, C. S.; Jornet-Somoza, J.; Mota, F.; Novoa, J. J.; Deumal, M. *J. Am. Chem. Soc.* **2010**, *132*, 17817−17830. (b) Deumal, M.; Rawson, J. M.; Howard, J. A. K.; Copley, R. C. B.; Robb, M. A.; Novoa, J. J. *Chem.—Eur. J.* **2010**, *16*, 2741−2750. (c) Deumal, M.; LeRoux, S.; Rawson, J. M.; Robb, M. A.; Novoa, J. J. *Polyhedron* **2007**, *26*, 1949−1958. (d) Awaga, K.; Tanaka, T.; Shirai, T.; Umezono, Y.; Fujita, W. *C. R. Chim.* **2007**, *10*, 52−57. (e) Preuss, K. E. *Dalton Trans.* **2007**, 2357−2369.

(7) (a) Rawson, J. M.; Alberola, A. In *Handbook of Chalcogen Chemistry. New Perspectives in Sulfur, Selenium and Tellurium*; Devillanova, F., Ed.; RSC Press: Cambridge, U.K., 2007. (b) Rawson, J. M.; Alberola, A.; Whalley, A. *J. Mater. Chem.* **2006**, *16*, 2560−2575. (c) Rawson, J. M.; Luzon, J.; Palacio, F. *Coord. Chem. Rev.* **2005**, *249*, 2631−2641. (d) Rawson, J. M.; Palacio, F. *Struct. Bond. (Berlin)* **2001**, *100*, 93−128.

(8) Oakley, R. T.; Reed, R. W.; Robertson, C. M.; Richardson, J. F. *Inorg. Chem.* **2005**, *44*, 1837−1845.

(9) (a) Blockhuys, F. In *Computational Methods in Science and Engineering. Advances in Computational Science*; Maroulis, G.; Simos, T. E., Eds.; American Institute of Physics: Woodbury, NY, 2009; Vol. *1*. (b) Tersago, K.; De Dobbelaere, C.; Van Alsenoy, C.; Blockhuys, F. *Chem. Phys. Lett.* **2007**, *434*, 200−204. (c) Tersago, K.; Van Alsenoy, C.; Woollins, D. J.; Blockhuys, F. *Chem. Phys. Lett.* **2006**, *423*, 422−426. (d) Tersago, K.; Oláh, J.; Martin, J. L. M.; Veszprémi, T.; Van Alsenoy, C.; Blockhuys, F. *Chem. Phys. Lett.* **2005**, *413*, 440−444.

(10) Oláh, J.; Blockhuys, F.; Veszprémi, T.; Van Alsenoy, C. *Eur. J. Inorg. Chem.* **2006**, 69−77.

(11) Sheldrick, G. M. *Acta Crystallogr., Sect. A: Found. Crystallogr.* **2008**, *64*, 112−122.

(12) (a) Spek, A. L. PLATON, A Multipurpose Crystallographic Tool, Version 10M; Utrecht University: Utrecht, The Netherlands, 2003. (b) Spek, A. L. *J. Appl. Crystallogr.* **2003**, *36*, 7−13.

(13) Macrae, C. F.; Edgington, P. R.; McCabe, P.; Pidcock, E.; Shields, G. P.; Taylor, R.; Towler, M.; van de Stree, J. *J. Appl. Crystallogr.* **2006**, *39*, 453−457.

(14) Stoll, S.; Schweiger, A. *J. Magn. Reson.* **2006**, *178*, 42−55.

(15) Frisch, M. J.; Trucks, G. W.; Schlegel, H. B.; Scuseria, G. E.; Robb, M. A.; Cheeseman, J. R.; Montgomery, J. A., Jr.; Vreven, T.; Kudin, K. N.; Burant, J. C.; Millam, J. M.; Iyengar, S. S.; Tomasi, J.; Barone, V.; Mennucci, B.; Cossi, M.; Scalmani, G.; Rega, N.; Petersson, G. A.; Nakatsuji, H.; Hada, M.; Ehara, M.; Toyota, K.; Fukuda, R.; Hasegawa, J.; Ishida, M.; Nakajima, T.; Honda, Y.; Kitao, O.; Nakai, H.; Klene, M.; Li, X.; Knox, J. E.; Hratchian, H. P.; Cross, J. B.; Adamo, C.; Jaramillo, J.; Gomperts, R.; Stratmann, R. E.; Yazyev, O.; Austin, A. J.; Cammi, R.; Pomelli, C.; Ochterski, J. W.; Ayala, P. Y.; Morokuma, K.; Voth, G. A.; Salvador, P.; Dannenberg, J. J.; Zakrzewski, V. G.; Dapprich, S.; Daniels, A. D.; Strain, M. C.; Farkas, O.; Malick, D. K.; Rabuck, A. D.; Raghavachari, K.; Foresman, J. B.; Ortiz, J. V.; Cui, Q.; Baboul, A. G.; Clifford, S.; Cioslowski, J.; Stefanov, B. B.; Liu, G.; Liashenko, A.; Piskorz, P.; Komaromi, I.; Martin, R. L.; Fox, D. J.; Keith, T.; Al-Laham, M. A.; Peng, C. Y.; Nanayakkara, A.; Challacombe, M.; Gill, P. M. W.; Johnson, B.; Chen, W.; Wong, M. W.; Gonzalez, C.; Pople, J. A. Gaussian 03, Revision B.05; Gaussian, Inc.: Pittsburgh, PA, 2003.

(16) Møller, C.; Plesset, M. S. *Phys. Rev.* **1934**, *46*, 618−622.

(17) Becke, A. D. *J. Chem. Phys.* **1996**, *104*, 1040−1046.

(18) Becke, A. D. *J. Chem. Phys.* **1993**, *98*, 5648−5652.

(19) (a) Perdew, J. P.; Burke, K.; Ernzerhof, M. *Phys. Rev. Lett.* **1997**, *78*, 1396−1396. (b) Perdew, J. P.; Burke, K.; Ernzerhof, M. *Phys. Rev. Lett.* **1996**, *77*, 3865−3868.

(20) (a) Petersson, G. A.; Al-Laham, M. A. *J. Chem. Phys.* **1991**, *94*, 6081−6090. (b) Petersson, G. A.; Bennett, A.; Tensfeldt, T. G.; Al-Laham, M. A.; Shirley, W. A.; Mantzaris, J. *J. Chem. Phys.* **1988**, *89*, 2193−2218.

(21) (a) McLean, A. D.; Chandler, G. S. *J. Chem. Phys.* **1980**, *72*, 5639−5648. (b) Krishnan, R.; Binkley, J. S.; Seeger, R.; Pople, J. A. *J. Chem. Phys.* **1980**, *72*, 650−654.

(22) (a) Davidson, E. R. *Chem. Phys. Lett.* **1996**, *260*, 514−518. (b) Peterson, K. A.; Woon, D. E.; Dunning, T. H. *J. Chem. Phys.* **1994**, *100*, 7410−7415. (c) Woon, D. E.; Dunning, T. H., Jr. *J. Chem. Phys.* **1993**, *98*, 1358−1371. (d) Kendall, R. A.; Dunning, T. H., Jr.; Harrison, R. J. *J. Chem. Phys.* **1992**, *96*, 6796−6806. (e) Dunning, T. H., Jr. *J. Chem. Phys.* **1989**, *90*, 1007−1023.
(23) (a) Strelets, B. Kh.; Efros, L. S. *Khim. Geterotsikl. Soedin.* **1969**, 565−566. (b) Huestis, L. D.; Walsh, M. L.; Hahn, N. *J. Org. Chem.* **1965**, *30*, 2763−2766.
(24) (a) Akulin, Yu. I.; Gel'mont, M. M.; Strelets, B. Kh.; Efros, L. S. *Khim. Geterotsikl. Soedin.* **1978**, 912−916. (b) Akulin, Yu. I.; Strelets, B. Kh.; Efros, L. S. *Khim. Geterotsikl. Soedin.* **1975**, 275−275.
(25) Bauer, H. *Ber.* **1913**, *46*, 92−98.
(26) (a) Mantina, M.; Chamberlin, A. C.; Valero, R.; Cramer, C. C.; Truhlar, D. J. *J. Chem. Soc. A* **2009**, *113*, 5806−5812. (b) Allen, F. H.; Kennard, O.; Watson, D. G.; Brammer, L.; Orpen, A. G.; Taylor, R. *J. Chem. Soc. Perkin Trans. 2* **1987**, S1−S19.
(27) (a) Cordero, B.; Gomez, V.; Platero-Prats, A. E.; Reves, M.; Echeverria, J.; Cremades, E.; Barragan, F.; Alvarez, S. *Dalton Trans.* **2008**, 2832−2838. (b) Tersago, K.; Mandado, M.; Van Alsenoy, C.; Bagryanskaya, I. Yu.; Kovalev, M. K.; Makarov, A. Yu.; Gatilov, Yu. V.; Shakirov, M. M.; Zibarev, A. V.; Blockhuys, F. *Chem.—Eur. J.* **2005**, *11*, 4544−4551. (c) Vilkov, L. V.; Mastryukov, V. S.; Sedova, N. I. *Determination of Geometrical Structure of Free Molecules*; Khimia Publishers: Leningrad, USSR, 1978.
(28) (a) Zibarev, A. V.; Bagryanskaya, I. Yu.; Gatilov, Yu. V.; Shchegoleva, L. N.; Dolenko, G. N.; Furin, G. G. *Khim. Geterotsikl. Soedin.* **1990**, 1683−1688. (b) Awere, E. G.; Burford, N.; Haddon, R. C.; Parsons, S.; Passmore, J.; Waszczak, J. V.; White, P. S. *Inorg. Chem.* **1990**, *29*, 4821−4830.
(29) (a) Chen, Z.; Wannere, C. S.; Corminboeuf, C.; Puchta, R.; Schleyer, P. v. R. *Chem. Rev.* **2005**, *105*, 3842−3888. (b) Schleyer, P. v. R.; Maerker, C.; Dransfeld, A.; Jiao, H.; Hommes, N. J. R. v. E. *J. Am. Chem. Soc.* **1996**, *118*, 6317−6318.
(30) (a) Bzhezovsky, V. M.; Kalabin, G. A. In *Chemistry of Organic Sulfur Compounds*; Belenky, L. I., Ed.; Khimia Publishers: Moscow, Russia, 1988. (b) Belton, P. S.; Woollins, J. D. *Magn. Reson. Chem.* **1986**, *24*, 1080−1082.
(31) Aitken, R. A.; Arumugam, S.; Mesher, S. T. E.; Riddell, F. G. J. *Chem. Soc., Perkin Trans. 2* **2002**, 225−226.
(32) Gassmann, J.; Fabian. *J. Magn. Reson. Chem.* **1996**, *34*, 913−920.
(33) Dust, J. M.; Arnold, D. R. *J. Am. Chem. Soc.* **1983**, *105*, 1221−1227.
(34) Jose, D.; Datta, A. *Cryst. Growth Des.* **2011**, *11*, 3137−3140.
(35) Huestis, L.; Emery, I.; Steffensen, E. *J. Heterocycl. Chem.* **1966**, *3*, 518−520.

dx.doi.org/10.1021/ic302203t | *Inorg. Chem.* 2013, 52, 3699−3710